# Effect of Swirl Preset Vorticity on Combustion Performance of Lobe Nozzle Combustor Chamber

*WANG Lijun**, *JIANG Jintao*, *YUAN Weiwei*, *MEN Kuo*, *XU Yijun*

College of Energy and Environment, Shenyang, Shenyang Aerospace University, Shenyang 110136, P.R. China

(Received 5 July 2018; revised 6 December 2018; accepted 13 December 2018)

**Abstract:** To improve the combustor performance of multi-point injection combustion, lobe nozzle design was applied to the aero-engine model combustor, by presetting the swirl through a certain twisted angle of the edge of the lobe outlet. Numerical simulation in combination with modelling test is used in this paper. The effects of swirl vorticity presetting onto the vortex structure, the characteristics of combustion temperature field, the combustor exit temperature field quality, the combustion efficiency, and the $NO_x$ emissions of multi-point injection combustion chamber are investigated. Compared with the conventional vortex flow at the lobe outlet edge, the results of numerical simulation and water modelling test of the swirl vorticity presetting show that the swirl presetting can efficiently enhance the range and intensity of the lobe-induced vorticities. Besides, it can improve the uniformity of the combustion temperature in the combustor chamber, together with the reduced emissions of the pollutant $NO_x$. Moreover, compared with the conventional lobe nozzle chamber, the swirl vortex presetting can effectively improve its combustion performance. The flow simulation test results demonstrate the fluid vortex structure in the combustion chamber and validate the simulation results.

**Key words:** lobe nozzle; vortex structure; multi-point injection; combustor chamber; combustion performance; combustion characteristics

**CLC number**: TK474 **Document code**: A **Article ID**: 1005-1120(2019)05-0828-10

## 0 Introduction

Combustion chambers in modern aero engines use a strong swirl to promote the mixing of fuel with air, to create a combustion stability zone and to improve the performance of the combustion chamber. The swirling vortex should be considered in the design of advanced combustion chambers. The lobe nozzle with a special geometry can induce downstream vortex structures such as streamwise vortex and normalized vorticities on the circular edge of its outlet, thereby efficiently mixing fluids over short distances[1-2]. For instance, the successful application of a lobe mixer has effectively improved the propulsion performance of aerospace in aerospace power plants. Presz et al.[3-4] proposed the concept of a mixer with a lobe nozzle. The experimental results showed that the ability of the lobe mixer to eject secondary streams was enhanced, compared with the traditional form of outlet. Yu et al.[5-6] concluded that there are two reasons for the formation of the flow vorticities in the lobe mixer, i.e., the radial pressure distribution induced by the special geometry of lobes at the outlet edge and the gap between the crest of the lobe and the inner wall of the nozzle. Meslem et al.[7] conducted experiments on different outlet shapes and found that semi-circular together with vertical wall configurations have higher mixing efficiency in the near field downstream of the lobe. Even in the millimeter-sized lobe mixer combustor, there is a strong formation and development of the fluid vortex. Moreover, the fluid vortex disappears quickly[8-9] due to the rapid expansion of the combus-

*Corresponding author, E-mail address: wanglijun@sau.edu.cn.

**How to cite this article**: WANG Lijun, JIANG Jintao, YUAN Weiwei, et al. Effect of Swirl Preset Vorticity on Combustion Performance of Lobe Nozzle Combustor Chamber[J]. Transactions of Nanjing University of Aeronautics and Astronautics, 2019,36(5):828-837.

http://dx.doi.org/10.16356/j.1005-1120.2019.05.014

tion gas. So far, numerical simulation techniques has been extensively used to investigate the flow and combustion characteristics of microwave valve lobe nozzle, circular cylindrical combustors and their influencing factors[10].

Lobe nozzle is used herein to design the combustion chambers for aero engines. The fuel is directly injected through a distributed array of fuel nozzles and is straightly injected into the vortex array induced by the circular edge of lobe nozzle, to improve the lean oil/air mixing rate, atomization and evaporation characteristics produced by the fuel distribution of multi-point injections. The lobe nozzle adopts two designs, the twist and non-twisted ones, named as the conventional lobe and the preset vorticity lobe to explore the effect of the pre-rotation flow induced by the outlet edge torsion on the combustion characteristics and combustor performance of the lobe nozzle combustion chamber. Compared with the conventional non-twisted lobe nozzle, this study was to improve the combustion characteristics and properties of the combustion chamber in combination with experiments. The effects of swirl vorticity presetting onto the vortex structure of the lobe nozzle induced, the combustion multi-physical quantity field, the combustion characteristics, and the feasibility of the lobe nozzle are applied to the aero engine combustion chamber design.

# 1 Models and Methods

## 1.1 Design of combustion chamber model

Fig.1 shows the geometric model of lobe nozzle combustion chamber. The combustion chamber consists of an air lobe, a distributed array of direct fuel nozzles, and a tapered square chamber body. The exit edge of the lobe nozzle is set at the inlet of the combustion chamber, and the right side view is the trailing edge profile of the lobe nozzle. Conventional and vorticity presetting lobe nozzles have the internal and external opening angles of 19.3° and 24.2°, respectively. In light of this, the vorticity presetting lobe was referred to the work by Ruetten[11] and twisted the lobe trailing edge of the conventional lobe nozzle counterclockwise by 8.4°. After the air

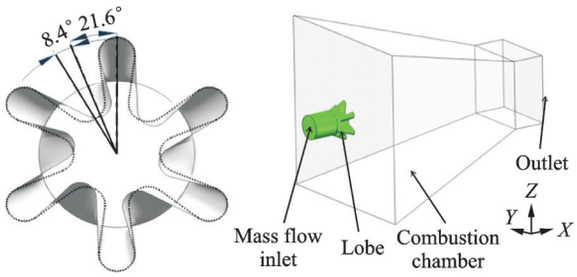


Fig.1 Model of lobe combustor chamber

is injected from the twist lobe nozzle, the presetting vorticities rotating counterclockwise work as an entire system when they enter the combustion chamber, where the flow direction is along the $X$ positive direction.

Fig.2 shows the installation positions and arrays of the multi-injection fuel nozzles on the lobe in the two types of combustion chambers. The fuel nozzles array is installed on the outlet section of the lobe and the fuel injects into the combustion chamber through the fuel nozzle array, as shown in Fig.2(a). Both fuel chambers use 13 fuel nozzles, which are uniformly distributed in the 6 flaps of lobe nozzle. The array arrangement is shown in Figs.2 (b), (c).

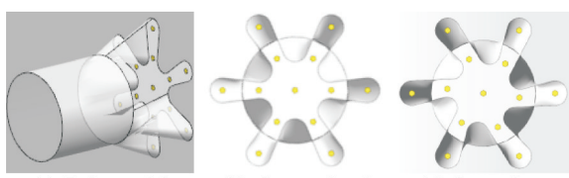


Fig.2 Fuel nozzle installation position and array mode

## 1.2 Physical model

Compared the experimental flow field with calculations results, different turbulence models were used to approach its applicability[12-16]. This paper selected the realizable two-equation turbulence model and the standard wall function to describe the turbulent flow of lobe nozzle. The probability density function (PDF) in the gas-liquid non-premixed combustion model was used to simulate the interaction of chemical reactions with turbulent flow. Multi-step chemical reaction models were depicted by using equilibrium chemical models. Discrete phase model (DPM) is used to simulate the discrete phas-

es of the kerosene particles in the flow field to account for complex factors, such as turbulent flow, complex chemical reactions, and their coupled turbulent flow. When the governing equations are discrete, the pressure terms are in a standard format, including kinetic energy terms, turbulence terms, and among others that are all in the high-order upwind style. The semi-implicit method for pressure linked equations-consistent (SIMPLEC) algorithm with convergence tolerance of $10^{-6}$ was used in the speed and pressure coupling.

### 1.3 Grid independence test

The ANSYS 17.0 software was used to perform ICEM meshing of the entire computational domain. Unstructured composite grids were used due to the structural complexity of the lobe nozzles. The wall uses a five-layer Prim boundary layer mesh. Table 1 shows the grid independence test results, where the calculation condition is depicted in Case 1 listed in Table 2. The grid independence test results in Table 1 shows that the results obtained using three different numbers of grids are relatively close, and the differences between the latter two are smaller. It also can be seen from Fig.3 that the difference between the latter two vorticity values is smaller. Taking the calculation results, the calculation accuracy and the computational time into account, the total number of grids is approximately 2.8 million.

**Table 1 Verification results of grid independence**

| Number of grids/ million | Average outlet speed/(m·s$^{-1}$) | Average outlet temperature/ K |
|---|---|---|
| 2.4 | 46.08 | 1 328.3 |
| 2.8 | 42.17 | 1 364.3 |
| 3.2 | 40.83 | 1 369.6 |

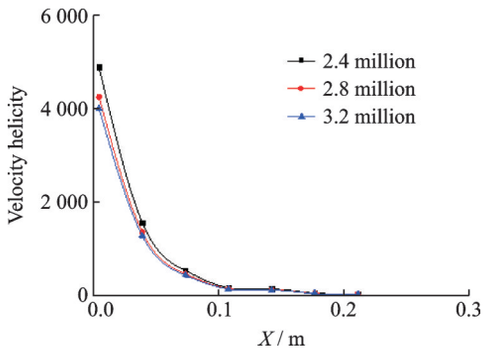


Fig.3 Streamwise vortex variation along the flow direction

### 1.4 Calculation conditions

According to NASA's typical test results of multi-point injection model combustion chamber[17-18], five of them were selected as the operating conditions for the test and simulation in this paper. The calculation conditions are shown in Table 2. The fuel injection conditions are the same for all working conditions. For each working condition, only the mass flow of air is changed, the fuel flow rate is equal to $7.670\times10^{-6}$, and the fuel temperature is set to 580 K. For each working condition of the lobe nozzle, the numerical analysis of the cold flow field vortex system, the combustion of multiple physical quantities, and the combustion performance of the combustion chamber model are carried out separately. The vortex of the flow simulations of some conditions were observed to verify the credibility of calculations. The effect of vorticity presetting on the flow combustion characteristics and combustion chamber performance were analyzed via the design of two kinds of lobe nozzle combustion chambers under five working conditions. The lobe combustor condition is simulated with mass flow inlet and pressure outlet.

**Table 2 Calculation conditions**

| Condition | Fuel/air ratio | Inlet mass flow/ (kg·s$^{-1}$) | Temperature/ K | Inlet pressure/ MPa | Combustion chamber pressure/ MPa |
|---|---|---|---|---|---|
| Case 1 | 0.025 | 0.030 43 | 827.59 | 1.723 | 1.654 |
| Case 2 | 0.026 | 0.029 26 | 827.59 | 1.723 | 1.654 |
| Case 3 | 0.029 | 0.026 23 | 827.59 | 1.723 | 1.654 |
| Case 4 | 0.031 | 0.024 54 | 827.59 | 1.723 | 1.654 |
| Case 5 | 0.035 | 0.021 73 | 827.59 | 1.723 | 1.654 |

## 2 Analyses of Flow Characteristics

### 2.1 Effect of swirl vorticities presetting on the vortex structure

The flow analysis concentrates on the vortical flow induced by the lobed nozzles. For vortex detection, different techniques for assignment and evaluation criteria are used. The normalized helicity density criterion Levy[19] is applied to identify vorticities, since it can distinct the co- and counter-rotating vortical flows, which is superior to others, for instance, the work of Jiang et al.[20] or Haller et al.[21]. By utilizing this criterion, the generation and development of the complex vorticities can be traced to provide an overview on main flow structures.

$$\omega = \nabla \bullet u$$
$$H = u \bullet \omega \tag{1}$$

where $u$ is the speed and $H$ is the velocity helicity.

In Fig.4, iso-surfaces are used to describe the streamwise vortex structure at the exit of the lobes. The velocity helicity is used to characterize the magnitude of the vorticity value. The main structure and development status of the downstream vortex of the two lobe nozzle designs can be observed intuitively. In Figs.4 (a, b), the iso-surfaces of $-300$ and $+300$ are extracted to illustrate the counter-clockwise and clockwise rotating flows in green and red, respectively. The streamwise vortex structures of the two lobe nozzles are induced in pairs on the round trailing edge of the lobe with the opposite direction. Under the action of the mainstream, the vortex structure gradually spreads outward and the range of action increases. With the enhanced swirling effect by the induced round edge of twisted outlet, an overall rotation and mutual entanglement are produced, as shown in $A$ in Fig.4 (b), compared with the conventional vorticity in Fig.4 (a). Fig.5 depicts the variation of the vorticity mean value along the flow direction of the combustion chamber. In Fig.5, the numerical values of streamwise vortex in the combustion chamber of both lobe nozzles reach the maximum at the exit of the lobe nozzle and plunge along the flow direction. When the fuel/air

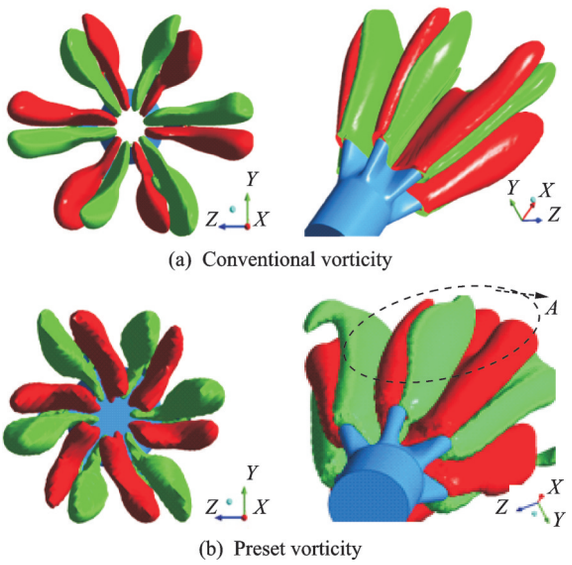


Fig.4 Streamwise vortex structure

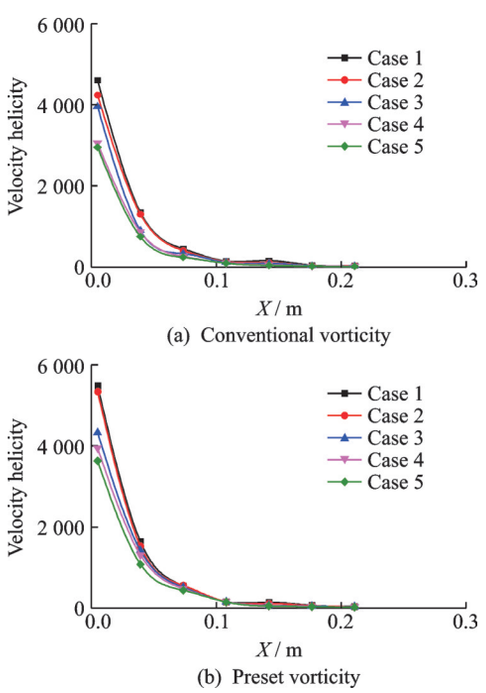


Fig.5 Streamwise vortex variation along the flow direction

ratio increases, the vorticity becomes larger without significant changes under the calculation conditions. It is due to the frictional loss caused by the viscosity and the effect of swirling dissipation in small fluid micro-clusters in the fluid. In the combustion chambers with the two types of lobe nozzles, the vorticity in the combustion chamber with the vortex presetting are generally higher than that of the conventional non-presetting one. Taking Case 1 as an example, when the lobe outlet uses swirl presetting, the maximum vorticity value is equal to $6.526\times10^3$,

which increases by 42% compared with the $4.596\times10^3$ of conventional non-swirl vortex.

In the downstream of the trailing edge of the lobe, the flow interactions form a strong shear stress layer, and the K-H [22-23] perturbations induce a strong normalized vortex. The variation of the dimensionless normalized vorticities in the combustion chamber with or without the swirl vorticity presetting are shown in Fig. 6. The magnitude of the quadratic vorticities in the combustion chamber with the two kinds of lobe nozzles reaches to the maximum at the exit of the lobe nozzle. The subsequent vorticity strength shows complex degradation that rebounds several times in the flow direction, exhibiting relevance to the fuel/air ratio under each working condition. This means that it is influenced by the complex interaction between normalized vorticities and streamwise vortex in a turbulence system. On the other hand, due to the entrainment of the surrounding fluid by the flow vortex, a strong shear stress layer is formed between the jet and the surrounding air, which changes the regularity of the strength of the normalized vortex to some extent. When $0.05<X<0.107$, the convergence of normalized vorticities increases the eddy rebound and becomes a vortex convergence zone. When $x$ is larger than 0.107 m and the cross section is 0.210 m, with the development of flow, the friction of the fluid microclusters is intensified, and the loss of eddy current strength decreases. For the vorticity presetting, when the inlet flow rate is small, the larger the torsional inertia is, the greater the effect on the flow vortex, yielding the stronger vorticity rebound of the normalized vortex. Taking Case 1 as an example, the maximum normalized vorticity value of the vorticities presetting at the lobe outlet edge is 33.47, and the maximum normalized vorticity value of the conventional non-swirl presetting is 22.75, with 45% increasement approximately.

Despite streamwise vortex or normalized vortex, the calculation results show that the vortex preset increases the size and intensity in combustion chamber with the two kinds of lobe nozzle. But the influence of the vorticity preset on the streamewise vortex is less than that of the normalized vortex,

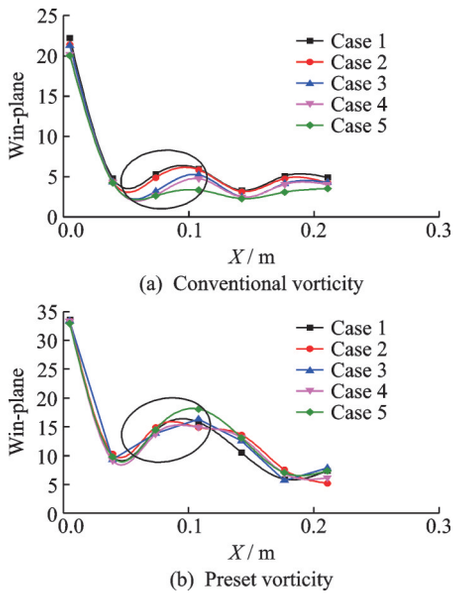


Fig.6 Normal vorticity variation along the flow direction

which is beneficial to the enhancement of the interaction between the vortex structures of the lobe.

## 2.2 Vortex structure tracer display test and verification of results

According to the similarity theory, the experimental setup is shown in Fig. 7. Using red ink as a tracer, the vortex structure downstream in the lobe is displayed. The water flows through the lobe nozzle into the combustion chamber and exits from the combustion chamber outlet. The two combustion chambers are different from the lobe nozzles. Fig. 8 shows the vortex structure traces of the conventional lobe and the vortex preset under Case 1 conditions. Figs. 8 (a), (b) depict observations of vortex structure test and numerical results of conventional lobe nozzle. Figs. 8 (c), (d) shows vortex structure test observation and numerical results of vortex lobe preset nozzle. Experimental observation and calculation is a part of vorticities at the corresponding side of outlet edge of the lobe nozzle. It can be seen from Fig. 8 that the vortex radially expands while spiraling along the axial direction of the combustion chamber. Because of the strong vortexes at the outlet, the neighbor fluid is sucked up, promoted to be mixed up and expanded gradually. The vorticities shown in Figs. 8 (b), (d) also rotated clockwise. The vorticities structure shown in Figs. 8 (c), (f) are also similar to experimental results. The evolu-

tion position of the vortex along the flow direction and the helical space expansion shape and range of the vortex are the same as the experimental one. For either the conventional vorticity or preset vorticity, comparison between experimental test and simulation results shows that the numerical simulation of the vortex system in terms of position, size, shape and spatial evolution is consistent with the experimental results. The spatial evolvable range of the vortex structure in the downstream direction of the preset vorticity is larger than that of the conventional vorticity, indicating that the preset vorticity has the function of expanding and twisting of the lobe vorticities. The consistency of numerical simulation and experimental results verifies the accuracy of numerical simulation.

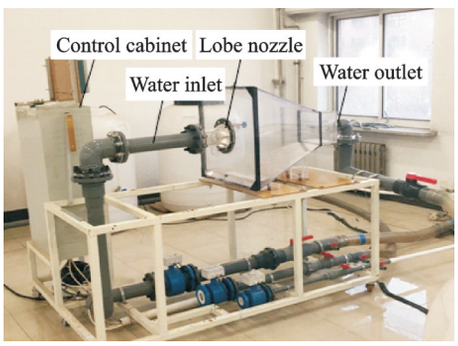


Fig.7 Water model test bench

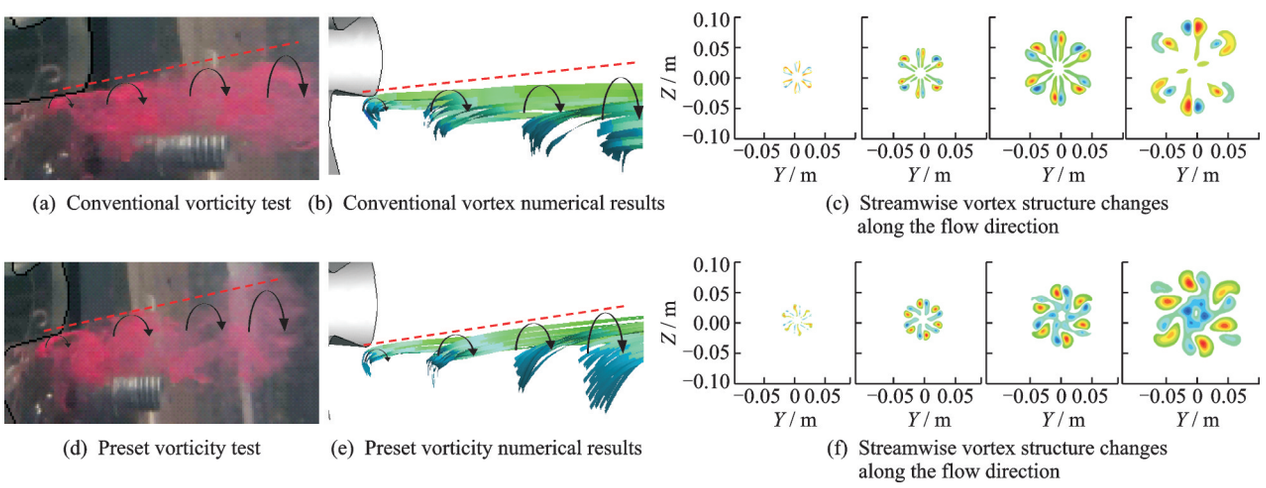


Fig.8 Effect of vorticity presetting on vortex structure in flow field

## 3 Analysis of Effect of Vorticities Presetting on Combustion Characteristics

### 3.1 Effect of vorticities presetting on combustion temperature field

Figs.9 (a—e) show a comparison of the combustion temperature field of the conventional central vortex and vorticity preset lobe combustors of cross-section under the five combustion conditions in Table 2. The upper half of each operating pattern stands for the conventional vortex combustion temperature field, and the lower half stands for that of the vorticity presetting. In Fig.9, under the effect of the vorticity preset, with the increasing fuel/air ratio, the flame centers in the combustor head are more dispersed along the radial direction, which represents a smaller gradient of the local combustion temperature field. With the increasing space for vorticity expansion, vorticity preset makes the expansion of the combustion zone more obvious when the fuel/air ratio increases. Moreover, the multi-point injection of fuel formed by the fuel nozzle arrangement results in the convergence of the distributed small flames generated under the twisting of the lobe vortex system, forming a downstream space combustion.

Figs. 10 (a—e) show the comparison of combustion temperature distribution along the axis with dashed line located 0.02 m up from centerline of combustion chamber, as shown in Fig.9. The black solid and the red dotted lines stand for the calculated

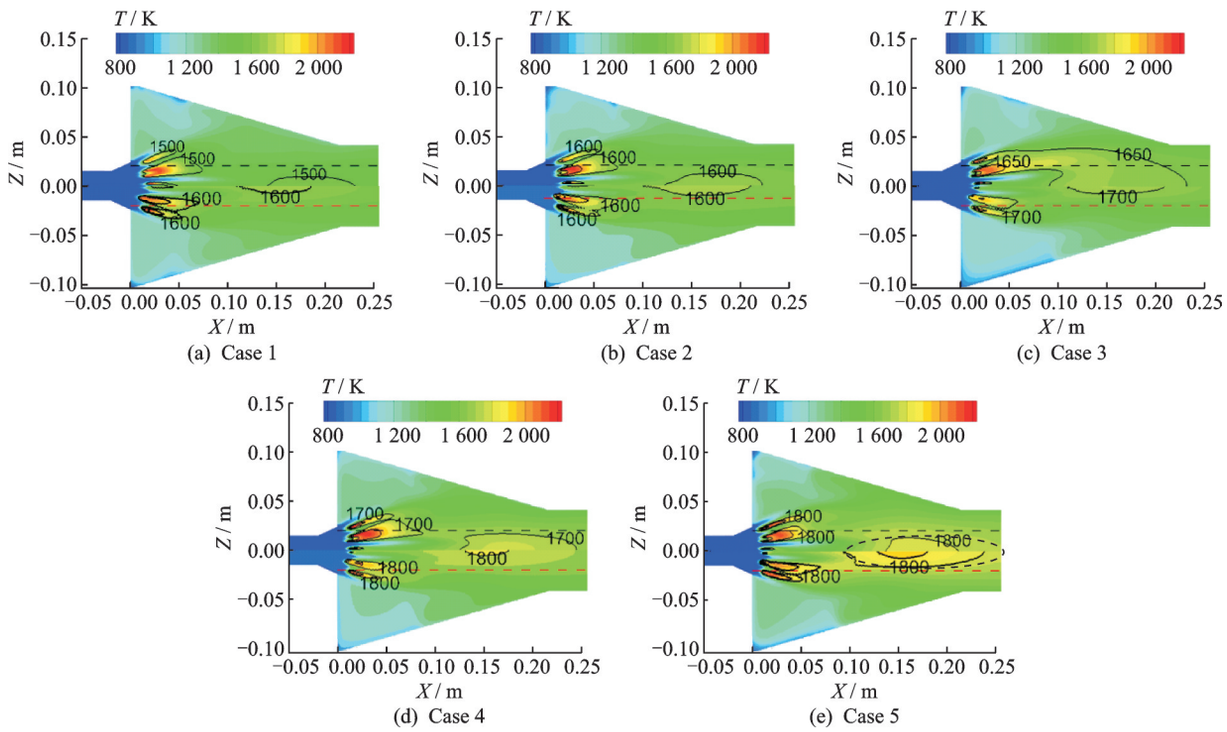


Fig.9 Effect of vorticity presetting on combustion temperature field

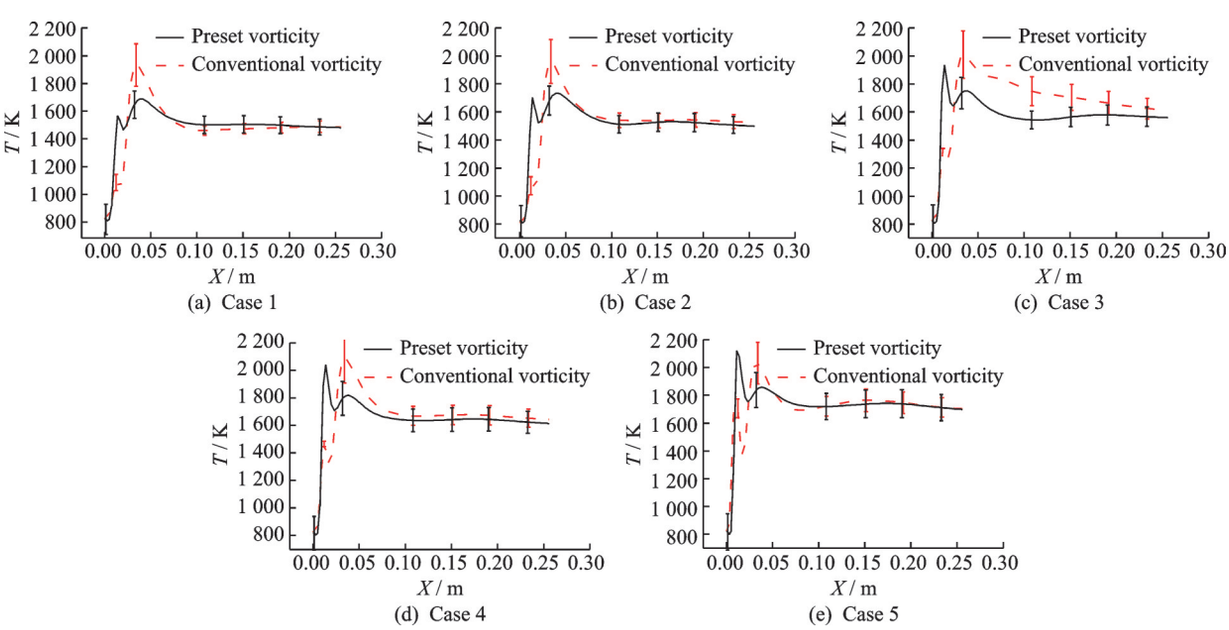


Fig.10 Temperature distribution along combustor centerline

results of the temperature distributions for the preset vorticity and the conventional vorticity, respectively. In Fig.10, preset vorticity reduces the maximum temperature variance and the average temperature at the head of the combustion chamber, compared with the conventional vorticity. The uniformity of the local combustion temperature distribution at combustion chamber head is improved. However, when the fuel/air ratio is relatively larger, the effect of the preset vorticity gradually decreases, which has the same effect of combustion in combustor chamber. The preset vorticity together with combustion behaves as a complicated coupling process.

### 3.2 Effect of vorticities presetting on the outlet temperature field quality

Outlet temperature distribution factor (OTDF) is defined as a performance parameter to

evaluate the exit temperature field quality of the combustion chamber. In the general design, the OTDF coefficient should be less than 0.35. The higher the quality of temperature field of outlet is, the more efficient the turbine blades work, and the longer the service life is.

Fig. 11 (a) shows the OTDF distribution for the two lobe nozzles of combustion chamber. In Fig.11 (a), both OTDF calculations with two lobe nozzles are much smaller than those of the general design. However, due to the presence of preset vorticity, temperature field in combustion chamber and OTDF with the lobe nozzle preset vorticity are more uniform than that of conventional lobe nozzle combustion chamber. Fig.11 (b) shows that, when the fuel/air ratio increases, the decreased preset vorticity will reduce the effect onto the quality improvement of the combustion temperature field at outlet.

### 3.3 Effect of vorticities presetting on combustion efficiency

Combustion efficiency is a performance index to evaluate whether the combustion of combustion chamber is completed. Both the geometry of the combustion chamber and the influence of chemical factors in the combustion process can lead to a reduction in combustion efficiency. The combustion efficiency is defined as

$$\eta = \left[1 - \frac{\mathrm{EI_{CO}LHV_{CO}} + \mathrm{EI_{CH_4}LHV_{CH_4}}}{1000\mathrm{LHV}}\right] \times 100\% \tag{2}$$

where EI is the pollutant emission index in the unit of g/kg, and LHV is the low calorific value in the unit of kJ/kg. The combustion efficiency calculation result is shown in Fig.11 (b). The combustion efficiency of the preset vorticity lobe nozzle is higher than that of the conventional lobe nozzle. Due to the effect of the preset vorticity, the vorticity value increases and the flow swirling is stronger, which is an important factor that makes the process of combustion more complete. Additionally, the combustion efficiency of the combustion chambers of both lobe nozzles gradually decreases with the increasing fuel/air ratio. Because of the increased fuel/air ratio, the decreased air flow leads to the reduced vorticity value and strength of the vortex structure. The decreased vortex strength has a negative effect on the mixed combustion process, which decreases the combustion efficiency.

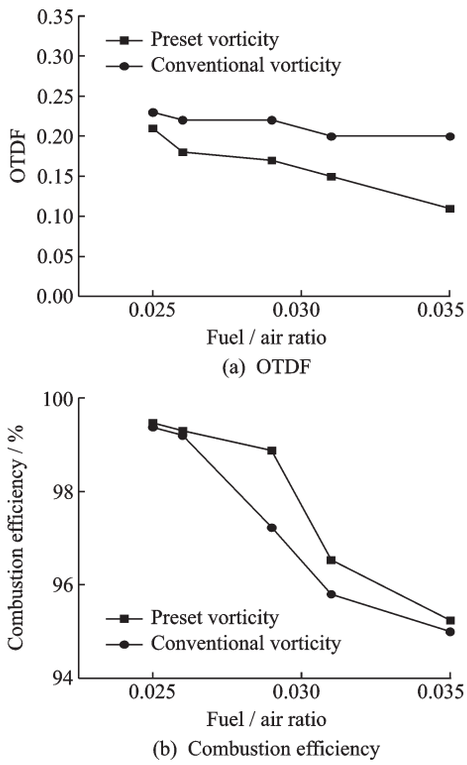


Fig.11 Effect of vorticity presetting on OTDF and combustion efficiency

### 3.4 Effect of vorticities presetting on total pressure recovery factor

Total pressure recovery coefficient refers to the ratio of the total pressure at the outlet of combustion chamber to the total pressure at the inlet. After the air flow passes through the combustion chamber, the total pressure of the air flow will decrease due to the viscosity of the gas and the temperature rise during the combustion process. Because of the significant spatial heterogeneity in the downstream flow in lobe nozzle combustion chamber, downstream flow blending introduces additional total pressure loss.

Total pressure recovery coefficient of the combustion chamber of the two lobe nozzles is shown in Fig. 12. The total pressure recovery coefficient of the combustion chamber with the preset vorticity lobe nozzle is smaller than that of the conventional

lobe nozzles. Preset vorticity enhances the interaction among vorticities, and it increases the additional total pressure loss, resulting in a lower total pressure recovery coefficient than the conventional lobe nozzle without vorticity presetting. Besides, the total pressure recovery coefficient gradually increases with the increasing fuel/air ratio due to the decreased vorticity intensity inlet ratio, since vorticity intensity at inlet decreases.

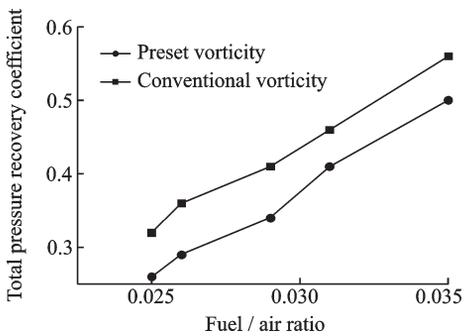


Fig.12 Total pressure recovery factor

### 3.5 Effect of vorticities presetting on combustion emissions

The calculated $NO_x$ emission from combustion chambers with two lobed nozzles is displayed in Fig.13. The $NO_x$ emission trends of the combustion chambers with two lobe nozzles are consistent, namely, it increases gradually with the increased fuel/air ratio, due to the reduced combustion efficiency and the increased mean value of temperature field in the combustor chamber. From the previous related analysis, $NO_x$ emission of conventional vorticity is higher than that of preset vorticity for its lower temperature distribution level.

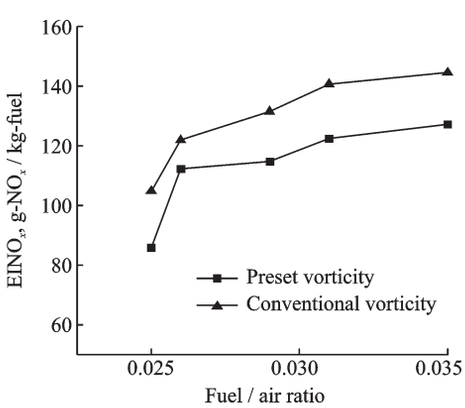


Fig.13 Effect of vorticity presetting on $NO_x$ emission

## 4 Conclusions

(1) The preset vorticity design can effectively increase the vorticity value in the vortex structure downstream of the lobe nozzle, and it can increase the eddy intensity and distribution space of the flow field.

(2) The water flow similarity test showed the existence and development characteristics of the induced vortex structure at the exit of the lobe, which validated the simulation calculation results.

(3) Presetting vorticity extends the spatial combustion range of multi-point distributed lobe combustors with better combustion uniformity as well as the enhanced coupling of eddy current characteristics and fuel/air ratio in multi-point combustion process. With the improvement of the combustion efficiency and the quality of the outlet temperature field, the $NO_x$ emission decreases. The multi-physical fields, such as fluid flow and combustion temperature by vorticity preset lobe are improved more effectively than that of conventional case.

(4) Presetting vorticity can achieve good combustion performance of the lobe combustion chamber, but with relatively high pressure loss.

**Reference**

[1] SKEBE S A, PATERSON R W, BABER T J. Experimental investigation of three-dimensional forced mixer lobe flow field[C]//The 1st National Fluid Dynamics Conference. Cincinnati: [s.n.], 1988: 1999-2006.

[2] Yakinthos K, Missirlis D, Palikaras A, et al. Optimization of the design of recuperative heat exchangers in the exhaust nozzle of an aero engine[J]. Applied Mathematical Modelling, 2007, 31(11): 2524-2541.

[3] PRESZ W M, REYNOLDS G, MCCORMICK D C. Thrust augmentation using mixer ejector diffuser systems[C]//Aerospace Sciences Meeting and Exhibit. Reno: [s.n.], 1994: 1-10.

[4] Tew D E, Teeple B S, Waitz I A. Mixer-ejector noise-suppressor model[J]. Journal of Propulsion & Power, 2015, 14(6): 941-950.

[5] YU S C M, XU X G. Flow characteristics of a confined co-axial nozzle with a central lobed mixer at different velocity ratios: AIAA-1997-1811[R]. [S.l.]: AIAA, 1997.

[6] YU S C M, XU X G. Confined coaxial nozzle flow

with central lobed mixer at different velocity ratios[J]. AIAA Journal, 36(3):349-358.

[7] MESLEM N A. Vortex dynamics and mass entrainment in turbulent lobe jets with and without lobe deflection angles[J]. Experiments in Fluids, 2010, 48(4): 693-714.

[8] Bin L U, Zhang J, Yong S, et al. Model experiment on mixing and combustion of lobed forced mixer[J]. Journal of Nanjing University of Aeronautics & Astronautics, 2017, 49(3):370-375.

[9] LIU Youhong. Numerical study of streamwise vortex formation in micro-lobed burners[J]. Journal of Aerospace Power, 2007(6): 859-863.

[10] XIE Yi, ZHONG Chen, YUAN Dengfang, et al. Combustion characteristics of micro-lobed burners[J]. Journal of Northeastern (Natural Science), 2017(4): 536-541.

[11] RUETTEN M, WOLDEGIORGIS F. Vortical flow structure genesis of lobed nozzle flows[C]//AIAA Fluid Dynamics Conference. [S.l.]: AIAA, 2016.

[12] COOPER N J, MERATI P, HU Hui. Numerical simulation of the vertical structures in a lobed jet mixing flow: AIAA-2005-635[R]. [S.l.]: AIAA, 2005.

[13] XIE Yi, LI Teng, LIU Youhong. Numerical investigation of vertical structured in a jet mixing flow of lobed mixer[J]. Science Technology and Engineering, 2011, 11(32): 7972-7978.

[14] LEI Zhijun. Experimental study on the mixing meechanisms of lobed mixer with inlet swirl in model turbofan engines[D]. Beijing: Chinese Academy of Science, 2010: 6-20.

[15] HU H, SAGA T, KOBAYASHI T. Dual-plane stereoscopic PIV measurements in a lobed jet mixing flow[C]//AIAA Aerospace Sciences Meeting & Exhibit. [S.l.]: AIAA, 2005.

[16] SHAN Y, ZHANG J Z. Numerical investigation of vortical structures in the lobed mixer-ejector[J]. Acta Aerodynamica Sinica, 2005, 23(3): 355-359.

[17] GOEKE J, PACK S, ZINK G, et al. Multi-point combustion system: NASA/CR-218112[R]. [S.l.]: NASA, 2014.

[18] TACINA R, MAO C P, WEY C. Experimental investigation of a multiplex fuel injector module for low emission combustors: AIAA 2004-0185[R]. [S.l.]: AIAA, 2004.

[19] DEGANI D, SEGINER A, LEVY Y. Graphical visualization of vortical flows by means of helicity[J]. AIAA Journal, 1990, 28(8): 1347-1352.

[20] JIANG M, MACHIRAJU R, THOMPSON D. Detection and visualization of vorticities[C]// Proceedings of IEEE Visualization. [S.l.]: IEEE, 2002: 307-314.

[21] HALLER G. On objective definition of a vortex[J]. J Fluid Mech, 2005, 525: 1-26.

[22] MAO R, YU S C M, ZHOU T, et al. Kelvin Helmholtz and streamwise vorticities in the near wake of a single-lobe forced mixer[J]. Journal of Engineering, 2006, 220(4): 279-298.

[23] Mc CORMICK D C, BENNETT J C. Vortical and turbulent structure of a lobed mixer free shear layer[J]. AIAA Journal, 2012, 32(9): 1852-1859.

**Acknowledgement** This work was supported by the Natural Science Fund of Liaoning Province Project (No. 201602566).

**Authors** Dr. **WANG Lijun** received his Ph.D. degree of Thermal Energy and Power Engineering in 2004. Now he is an associate professor of Shenyang Aerospace University. His research focuses on aviation engine combustion chamber design and analysis, engineering thermal physics and other research.

Mr. **JIANG Jintao**, Mr. **YUAN Weiwei**, Mr. **MEN Kuo**, and Mr. **XU Yijun** are all postgraduate students of Shenyang Aerospace University. Their research interest focuses on simulation of combustion flow.

**Author contributions** Associate Prof. **WANG Lijun** designed the study, complied the models, conducted the CFD simulation, experiments and analysis, and revised the manuscript. Dr **JIANG Jintao** contributed to the simulation and experiments data and wrote the manuscript. Mr. **YUAN Weiwei**, **MEN Kuo**, and **XU Yijun** participated in experimental sample collection and some figures generation. All authors commented on the manuscript draft and approved the submission.

**Competing interests** The authors declare no competing interests.

(Production Editor: Zhang Tong)